Food Chemistry 383 (2022) 132545

Contents lists available at ScienceDirect

Food Chemistry

journal homepage: www.elsevier.com/locate/foodchem

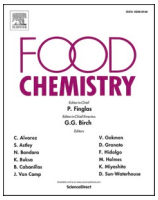

Non-invasive monitoring of *in vitro* gastric milk protein digestion kinetics by ^{1}H NMR magnetization transfer

Morwarid Mayar [a,b], Julie L. Miltenburg [c], Kasper Hettinga [c], Paul A.M. Smeets [b,d], John P. M. van Duynhoven [a,*], Camilla Terenzi [a]

[a] *Laboratory of Biophysics, Wageningen University, Wageningen, The Netherlands*
[b] *Division of Human Nutrition and Health, Wageningen University, Wageningen, The Netherlands*
[c] *Food Quality and Design, Wageningen University, Wageningen, The Netherlands*
[d] *Image Sciences Institute, University Medical Center Utrecht, Utrecht University, Utrecht, The Netherlands*

ARTICLE INFO

Keywords:
Protein digestion
^{1}H NMR
Magnetization transfer
Skim milk
Casein coagulation
Two-pool exchange

ABSTRACT

Processing of milk involves heating, which can modify the structure and digestibility of its proteins. *In vitro* models are useful for studying protein digestion. However, validating these models with *in vivo* data is challenging. Here, we non-invasively monitor *in vitro* gastric milk protein digestion by protein-water chemical exchange detected by ^{1}H nuclear magnetic resonance (NMR) magnetization transfer (MT). We obtained either a fitted composite exchange rate (*CER*) with a relative standard error of $\leq$10% or the MT ratio (*MTR*) of the intensity without or with an off-resonance saturation pulse, from just a single spectral acquisition. Both *CER* and *MTR*, affected by the variation in the amount of semi-solid protons, decreased during *in vitro* gastric digestion in agreement with standard protein content analyses. The decrease was slower in heated milk, indicating slower breakdown of the coagulum. Our results open the way to future quantification of protein digestion *in vivo* by MRI.

1. Introduction

Protein intake is essential for the growth and repair of body cells, muscle function and development of the immune system. Milk is one of the main food sources of protein in the human diet. Gastric digestion is the first step in the breakdown of milk proteins, namely casein and whey proteins, and in the subsequent absorption of amino acids (Walstra, Wouters, Geurts, 2006). However, industrial preparation of milk products includes heating, which can modify the structure and the gastric digestibility of the proteins. Understanding the effect of heating on protein digestion can ultimately aid in optimizing the industrial processing of milk proteins. During gastric digestion, gastric acid and pepsin cause aggregation of the casein micelles into a semi-solid casein coagulum, followed by subsequent hydrolysis of the proteins by pepsin (Egger et al., 2019; Nakai & Li-Chan, 1987). Due to their open structure, caseins are almost completely broken down into peptides in the gastric phase, while native whey proteins are more resistant to hydrolysis due to their globular structure, and are still largely intact after gastric digestion (van Lieshout, Lambers, Bragt, & Hettinga, 2020). The modifications imposed on the proteins during heating can affect both the structure of the coagulum and the digestion of caseins and whey proteins (Mulet-Cabero, Mackie, Wilde, Fenelon, & Brodkorb, 2019).

Protein digestion is commonly studied using static or dynamic *in vitro* digestion models that in turn mimic either adult (Brodkorb et al., 2019; Dupont et al., 2019) or infant digestion (Ménard et al., 2018). During *in vitro* digestion studies, samples are taken at different digestion time points, and are typically analyzed with the o-phthalaldehyde (OPA) assay, sodium dodecyl sulphate–polyacrylamide gel electrophoresis (SDS-PAGE), high performance liquid chromatography (HPLC) and liquid chromatography coupled to mass spectrometry (LC-MS) (Egger et al., 2019; Macierzanka et al., 2012). These methods, limited to *in vitro* applications, typically only measure the supernatant instead of the whole digestion sample including the coagulum formed during phase separation. Whereas *in vitro* digestion studies can provide valuable insights into protein digestion kinetics and the chemical composition of the digesta, they do not fully capture the complexity of the digestive tract. *In vivo* studies provide a biological environment that is hard to replicate *in vitro* because the digestive tract is within a complex biological system containing delicate feedback controls. For instance, secretion of digestive juice in response to a meal is automatically

* Corresponding author.
E-mail address: john.vanduynhoven@wur.nl (J.P.M. van Duynhoven).

https://doi.org/10.1016/j.foodchem.2022.132545
Received 2 October 2021; Received in revised form 19 February 2022; Accepted 21 February 2022
Available online 24 February 2022

controlled *in vivo* but are difficult to reproduce through *in vitro* experiments (Bornhorst & Paul Singh, 2014). Moreover, the physicochemical conditions, such as pH, ionic strength and enzyme concentration evolve with time and influence digestion. Static *in vitro* digestion models do not take these evolutions over time into account. Protein digestion may be better understood through *in vivo* monitoring in humans, which can help optimize and validate the *in vitro* digestion models. Therefore, non-invasive techniques must be developed to monitor both *in vitro* and *in vivo* digestion.

Magnetic resonance imaging (MRI) is promising for studying *in vivo* protein digestion, because it can be used to study physiological processes in a non-invasive manner (Smeets, Deng, Van Eijnatten, & Mayar, 2020). MRI is based on nuclear magnetic resonance (NMR), which has been applied widely to characterize a variety of food systems, including milk and milk products (Bordoni et al., 2011; Duynhoven, Voda, Witek, & Van As, 2010; Le Dean, Mariette, & Marin, 2004). MRI is currently used to study gross changes in digesta, linked to changes in food structure and possible phase separation, by visual assessment of anatomical images of the stomach (De Zwart & De Roos, 2010; Spiller & Marciani, 2019). Yet, such images do not provide a local molecular-scale measure of the degree of protein coagulation and subsequent protein hydrolysis. It has already been established that it is possible to indirectly monitor the *in vitro* gastric digestion of whey protein gels by measuring the ^{1}H transverse relaxation time (T_2) of the supernatant, which changes during digestion due to a release of proteins and peptides from the gel (Deng et al., 2020). Contrarily to standard biochemical methods, all these NMR/MRI measurements are suitable for non-invasive studies in humans, and of whole digestion samples, in principle including both liquid and semi-solid phases. Yet, with T_2 studies it is not possible to capture the breakdown of coagulated caseins, especially in the early stages of digestion. This is because NMR spectrometers and clinical scanners cannot directly assess the short (μs-ms range) T_2 NMR relaxation times associated with semi-solid proteins. Magnetization Transfer (MT) is an NMR technique that is used to quantify low-abundant semi-solids dispersed in aqueous food matrices as a complementary method to T_2 relaxometry (Chinachoti, Vittadini, Chatakanonda, & Vodovotz, 2008; Duynhoven, Kulik, Jonker, & Haverkamp, 1999). This technique found widespread use in both pre-clinical and clinical MRI because of its potential to improve tissue contrast, compared to conventional MRI techniques, and its capacity to quantitatively characterize tissues in which biopolymers form semi-solid networks (Guo, Erickson, Trouard, Galons, & Gillies, 2003; Sled, 2018; Van Zijl et al., 2003).

In conventional NMR and MRI, only signals from mobile protons are detected that have sufficiently long T_2 relaxation times and are present at high concentrations. The T_2 of motion-restricted protons from semi-solid macromolecules, such as proteins, is too short to be detected directly by NMR spectrometers with long dead times of typically a few ms. MT enables indirect detection of protons from low-abundance semi-solid macromolecules, with short T_2 relaxation times, through the signal of the more mobile water protons.

In MT measurements, a radio frequency (RF) pulse with a specific amplitude and frequency is applied to saturate the magnetization of the protons associated with the semi-solid macromolecules by equilibrating the populations of the ^{1}H energy levels. The saturation is then transferred to the more mobile water ^{1}H via a combination of through-space dipolar interactions and ^{1}H exchange between the semi-solid macromolecules and water (Vlaardingerbroek & Boer, 2003). The saturation transfer can then be detected as a suppression of the water signal. The magnitude of the signal suppression is mainly dependent on the ^{1}H exchange rate and on the population of the semi-solid pool (Henkelman, Stanisz, & Graham, 2001). Since changes in the semi-solid protein pool occur during gastric milk protein digestion, which involves casein coagulation and digestion of both casein and whey proteins, we hypothesize that MT can be used to monitor these changes *in vitro*, on the whole digestion sample, via the ^{1}H protein-water exchange kinetics. The latter can be quantified by multi-parameter fitting of MT spectra recorded with different saturation pulse amplitudes and frequency offsets with respect to the signal of water. This approach enables the quantification of exchange and relaxation parameters of the liquid and semi-solid components (Henkelman et al., 1993). However, these measurements are time-consuming and, hence, not applicable to dynamic *in vivo* studies, where fast measurements are desired to meet safety requirements and avoid breathing motion artefacts in the images. Therefore, in clinical MRI, mostly a semi-quantitative rapid measurement of the MT ratio (*MTR*) is performed to obtain MT-contrast images. Signal saturation with at least one pulse amplitude and two frequency offsets is required in order to obtain the *MTR*. The *MTR* is a semi-quantitative parameter, because it depends not only on the rate of magnetization transfer, but also on the direct saturation of the water signal (Henkelman et al., 2001; Sinclair et al., 2010). In this study of *in vitro* gastric milk protein digestion, we validate and assess the quantification of protein-water exchange kinetics by MT during digestion, as well as the respective faster semi-quantitative *MTR* measurements, in view of their ultimate feasibility under *in vivo* conditions using MRI.

2. Materials and methods

2.1. Materials

Pepsin from porcine gastric mucosa (631 activity units/mg), pepstatin A, HCl, KCl, $NaHCO_3$, NaCl, Bis-Tris buffer, DL-dithiothreitol (DTT) and guanidine hidrochloride (GdnHCl) were purchased from Sigma Aldrich, Inc. (St. Louis, USA). o-phthalaldehyde (OPA), disodiumtetraborate decahydrate, sodiumdodecyl sulfate, tri-sodium citrate dihydrate, trifluoroacetic acid (TFA) were purchased from Merck (Darmstadt, Germany). HPLC ultra-gradient grade acetonitrile was purchased from Biosolve Chemicals (Valkenswaard, The Netherlands). Milli-Q water (resistivity 18.2 MΩ.cm at 25 °C, Merck Millipore, Billerica, USA) was used in all experiments.

2.2. Preparation of raw and heated skim milk

Raw cow's milk was provided by FrieslandCampina (Wageningen, The Netherlands). To obtain skim milk (SM), the raw milk was centrifuged at 6000 *g* for 20 min at 4 °C. The cream that was formed on top was removed and the remaining SM was stored at −20 °C. The heated SM samples were prepared by heating SM in a water bath at 80 °C or 70 °C for 30 min.

2.3. In vitro infant gastric protein digestion protocol

In vitro gastric digestion of raw and heated SM was conducted based on a digestion protocol for 1 month old infants (Ménard et al., 2018). This digestion protocol was chosen because milk protein digestion, and the effect of heating on digestion, is most poorly understood in infants. The methodology described in this paper can however directly be applied to other digestion models, such as Infogest (Brodkorb et al., 2019). First, simulated gastric fluid (SGF) and SM were separately heated in a water bath at 37 °C for 5 min. SGF was composed of NaCl and KCl with a concentration of 94 and 13 mM, respectively, and a pH of 5.3. Next, 1 mL of digestion sample was prepared by mixing SM and SGF containing pepsin in a 10-mm NMR tube in a 63:37 (v/v) ratio. The activity of pepsin in the digestion sample was 268 U/mL. The pH was adjusted to 5.3 with 1 M HCl. The samples were incubated in a water bath at 37 °C for t = 0, 1, 5, 15, 30 and 60 min. These time points were based on Ménard et al. (2018) with the addition of t = 1 min to better capture the fast disappearance of the coagulum in raw SM. The activity of pepsin was stopped by adding 10 μL of a 60 μmol/mL Pepstatin A solution to each of the prepared samples. The samples were measured by NMR without any further sample preparation.

2.4. NMR measurements

All the ^{1}H MT NMR measurements were conducted at a magnetic field strength of 7 T, corresponding to a ^{1}H frequency of 300.13 MHz, on an Avance III spectrometer (Bruker Biospin, Fällanden, Switzerland) equipped with a 10-mm diff30 probe. ^{1}H NMR spectra were acquired at room temperature with an MT pulse sequence, consisting of a continuous-wave (CW) saturation pulse followed by a 90° RF excitation pulse and acquisition of the free induction decay (FID) during the time *acq* ($CW(5s) - 90^{\circ}{}_x(13.5\mu s) - acq(0.4s)$). The recycle delay was set to 5 s, and 8 acquisitions were recorded with 8-step phase cycling. To obtain quantitative data, MT NMR spectra were measured using 29 different values of the frequency offset (Δ), ranging from 90 Hz to 130 kHz, and 3 values of the saturation pulse amplitude ($\omega_1/2\pi$), resulting in a total measurement time of 2 h. Single-point MT measurements were performed with $(\omega_1/2\pi), = 0.50$ kHz and $\Delta = 130$ and 7.5 kHz, resulting in a total acquisition time of 2.6 min.

2.5. Two-pool exchange model

The two-pool exchange model (Eq. (1)), consisting of a free water pool (A) and a semi-solid macromolecular pool (B), was used to fit the MT spectra obtained at different ω_1 and Δ:

$$\frac{M_Z^A}{M_0^A} = \frac{R_1^B \cdot \left[\frac{R_{ex}M_0^B}{R_1^A}\right] + \left(R_1^B + R_{rfB} + R_{ex}\right)}{\left[\frac{R_{ex}M_0^B}{R_1^A}\right] \cdot \left(R_1^B + R_{rfB}\right) + \left(1 + \left(\frac{\omega_1}{2\pi\Delta}\right)^2 \cdot \left[\frac{R_2^A}{R_1^A}\right]\right) \cdot \left(R_1^B + R_{rfB} + R_{ex}\right)} \quad (1)$$

where R_1 and R_2 are the longitudinal and transverse relaxation rates, respectively, R_{ex} is the chemical exchange rate constant and M_0^B is the population of the semi-solid pool. The R_{rfB} parameter is the RF absorption rate of the semi-solid pool and it depends on the absorption line shape of the restricted pool, which is typically described by a Gaussian function:

$$R_{rfB} = \omega_1^2 \cdot \sqrt{\frac{\pi}{2}} \cdot T_2^B \cdot e^{-\frac{\left(2\cdot\pi\cdot\Delta T_2^B\right)^2}{2}} \quad (2)$$

Four parameters were obtained from the fitting, namely: $R_{ex}M_0^B/R_1^A$, T_2^B, R_{ex}, and R_2^A/R_1^A. It is known from the literature that the model is weakly dependent on R_1^B and that it is not possible to obtain a precise estimate of this parameter from the model. Therefore, R_1^B was fixed to 1 s^{-1} (Morrison, Stanisz, & Henkelman, 1995). The $R_{ex}M_0^B/R_1^A$ and R_{ex} parameters are of particular interest for monitoring protein digestion, because they describe the ^{1}H protein-water exchange kinetics, which is expected to change during protein digestion. For simplicity and in analogy to *MTR*, in the following the $R_{ex}M_0^B/R_1^A$ parameter will be referred to as the composite exchange rate (*CER*).

2.6. Data processing and calculations

All processing and calculations were done in Matlab R2019b (MathWorks, Massachusetts, USA). Each magnitude spectrum was obtained as the absolute value of the respective complex spectrum after Fourier transformation of the free induction decays (FIDs). The maximum intensity of the water peak was calculated for the different ω_1 and Δ, which were subsequently used to calculate the S_{sat}/S_0 ratio. Global fitting of the S_{sat}/S_0 ratios was performed with the two-pool exchange model using the non-linear least squares method with the trust-region algorithm. The 95% confidence interval (CI) for each model parameter was determined via a bootstrap procedure with residual resampling and included 1000 repetitions (Efron & Tibshirani, 1993). To obtain a good estimate of the 95% CI for the *CER* from the one-datapoint fit, a Gaussian distribution of 1000 samples was simulated for the S_{sat}/S_0 obtained with $\omega_1/2\pi = 0.50$ and $\Delta = 7.5$ kHz. The standard deviation for the simulation was estimated from triplicate measurements of the S_{sat}/S_0. The simulated S_{sat}/S_0 ratios were separately fitted with the two-pool exchange model, resulting in 1000 values for *CER* from which the 95% CIs were calculated. All parameters in the model, except the *CER*, were fixed to their respective average value across the different digestion samples.

2.7. Protein content quantification

First the supernatant was separated from the coagulum by centrifuging the digestion sample at 10,000 *g* for 30 min. The white semi-solid protein coagulum was obtained as a result of phase separation occurring during *in vitro* protein digestion. Next, the soluble nitrogen content in the supernatant was quantified using a DUMAS Flash EA 1112 Protein analyzer (Thermo Fisher Scientific, Massachusetts, USA). A conversion factor of 6.38 was used to obtain the protein content from the nitrogen content. The coagulated protein fraction was calculated by subtracting the protein content in the supernatant from the total known amount of protein in the sample.

2.8. RP-HPLc

The total amount of caseins in the supernatant of the digestion samples was determined by RP-HPLC (Thermo Scientific™ UltiMate 3000, Massachusetts, USA) equipped with an Aeris Widepore 3.6 μm XB-C18 column, 250 × 4.6 mm (Phenomenex, the Netherlands), according to the method described by de Vries et al. (2015). Two solvents (A and B), consisting of 0.1% TFA in milliQ water (Millipore, Billerica, MA) and 0.1% TFA in acetonitrile, respectively, were used as the mobile phase for protein elution. The resulting chromatograms were analyzed with Chromeleon 7.1.2. (Thermo Fisher Scientific, Massachusetts, USA). The sum of the peak areas of α_{s1}-, α_{s2}-, β-, and κ-casein in the supernatant were determined for each of the digestion samples.

3. Results and discussion

3.1. MT spectra of raw and heated SM during in vitro gastric protein digestion

In vitro gastric digestion of SM was followed by recording MT spectra as a function of the frequency offset with $\omega_1/2\pi = 0.50$ kHz. Especially in the frequency offset range 2–10 kHz, the MT spectra of both raw (Fig. 1a) and heated (Fig. 1c) SM deviated from the reference sigmoid curve expected for a system, such as bulk water, devoid of MT effects. The observed shape was characteristic of a system containing a semi-solid macromolecular pool, similar to what has been observed for agar gels and membrane mixtures (Morrison et al., 1995). In such a system, MT is expected to occur between the NMR signal of semi-solid macromolecules and that of water via ^{1}H exchange.

A shift from high to low frequency offsets was observed in the MT spectra of raw SM with increasing digestion times (Fig. 1a). Large differences were observed between the MT spectra at t = 0 min and t = 1 min as well as between t = 1 min and t = 5 min. The shift in the MT spectra indicates that both the semi-solid proteins and the exchange rate decreased with increasing digestion time. The decrease in the amount of semi-solid proteins was also visible in the digestion samples (Fig. 1b). The photographs of the digestion samples showed that a physical separation occurred between a semi-solid pool that consisted of coagulated caseins and a supernatant that consisted of soluble proteins and peptides. Initially, casein coagulation takes place because the acidic environment during gastric digestion neutralizes the negative charge on the surface of the casein micelles. These neutralized casein micelles will interact with each other and form a coagulum. The formation of this casein micelle coagulum is known as acid-induced coagulation, which mainly leads to the formation of small flocs (Fig. 1b, t = 0 min) that can coagulate further into a bigger coagulum once pepsin is added. Pepsin

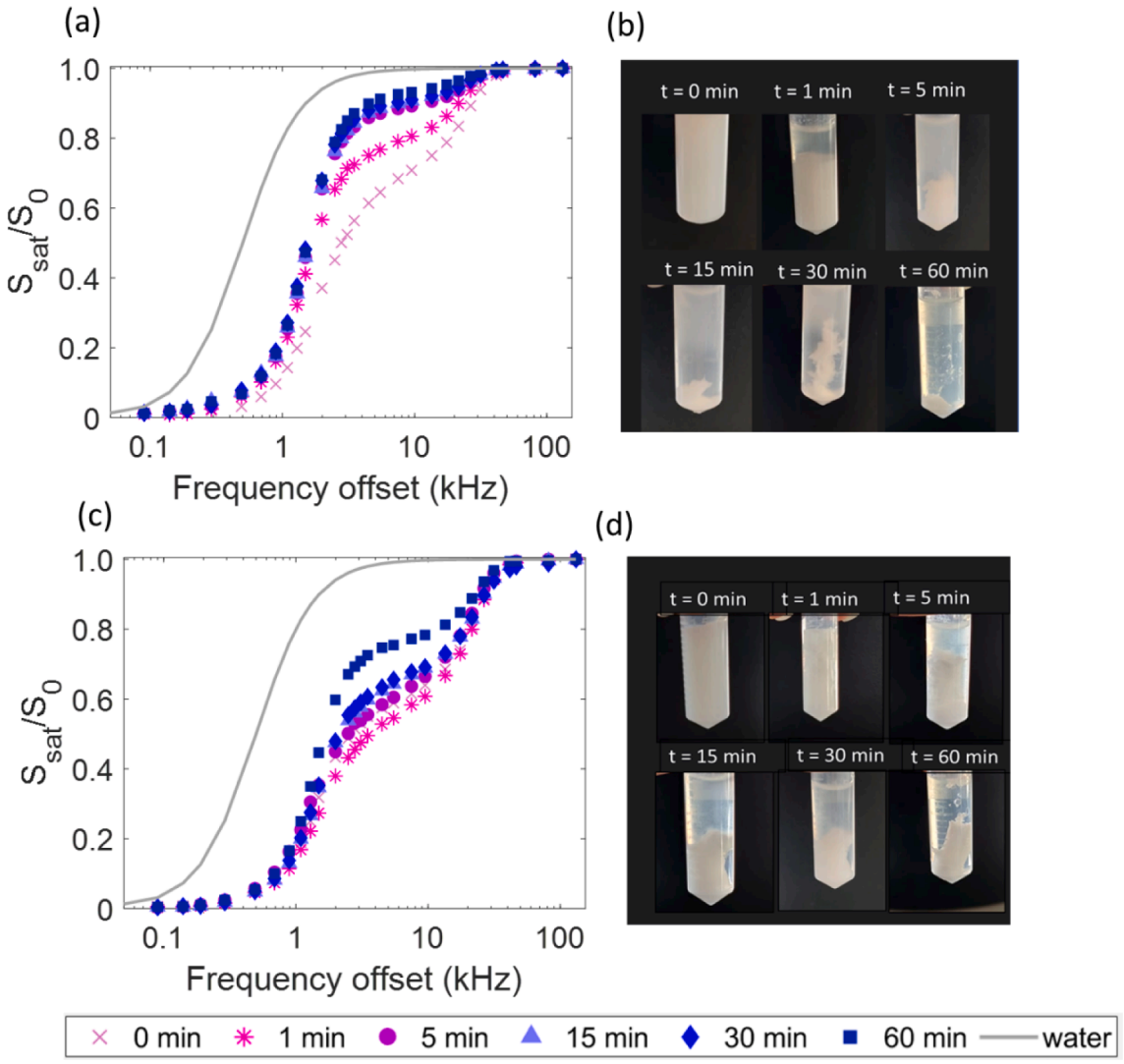

Fig. 1. Left: ^{1}H MT NMR spectra acquired with $\omega_1/2\pi = 0.50$ kHz for (a) raw skim milk and (c) skim milk heated at 80 °C (90% whey protein denaturation) digested in the *in vitro* infant gastric digestion model for t = 0, 1, 5, 15, 30 and 60 min. Right: photographs of the digestion samples of (b) raw and (d) heated skim milk, in which two phases can be distinguished, namely a precipitate consisting of the coagulum and a supernatant consisting of soluble proteins and peptides.

cleaves, amongst others, the κ-casein tails on the surface of the casein micelles, which leads to the formation of a tighter coagulum that can be macroscopically observed as a clot (Fig. 1b, t = 1 min). As the digestion continues, the casein coagulum is broken down by pepsin through hydrolysis of peptide bonds in all caseins (Didier Dupont & Tomé, 2014). This was observed in both the MT spectra and the photographs of the digestion samples. After t = 5 min, the MT spectra largely overlapped, with only small differences observed in the intermediate range of frequency offsets, namely 2–10 kHz, where the ^{1}H protein-water exchange is mostly captured. We note that the MT spectra were different from those of water, which indicates that even at t = 60 min still some semi-solid protein was present in the sample.

The protein coagulum in heated SM consists of both caseins and denatured WP. The MT spectra of heated SM (Fig. 1c) were notably different from those of raw SM (Fig. 1a). Lower S_{sat}/S_0 values and smaller differences between t = 0 and 30 min were observed for heated SM than for raw SM, especially in the frequency offset range 2–10 kHz. The most significant variation in the MT spectra of heated SM was observed between t = 30 and 60 min. This indicates that heating slows down the *in vitro* gastric digestion of the protein coagulum, which is in agreement with the photographs of the digestion samples (Fig. 1d). After 60 min of digestion, only a small amount of casein coagulum was present for raw SM, whereas for heated SM the amount of protein coagulum was similar to that of raw SM at t = 5 min. The heated SM sample was prepared by heating raw SM for 30 min at 80 °C, resulting in 90% WP denaturation, which is quite high. To explore whether MT can distinguish raw SM from heated SM with a lower WP denaturation level, we also measured heated SM with 27% WP denaturation (Fig. S1). These results showed that from t = 1 min onwards, the MT spectra of the three milk samples are distinctly different from each other. At t = 60 min, the MT spectra of the two heated milk samples overlap, but can still be distinguished from the respective spectrum of raw milk. Therefore, it is possible to study the effect of heating at different temperatures on the breakdown of the protein coagulum with MT.

3.2. *Multi-parameter fitting of MT spectra*

Protein digestion was quantitatively monitored by fitting MT spectra obtained at different $\omega_1/2\pi$ and Δ values with the two-pool exchange model (Henkelman et al., 1993). We also assessed the performance of three- and two-pool exchange with the inclusion of a dipolar order models, respectively containing 10 and 5 fitting parameters (data not shown) (Ceckler, Maneval, & Melkowits, 2001). As expected, fitting errors with the three-pool exchange model were very large, even for

simulated data. The two-pool exchange model with inclusion of a dipolar order contains one extra fitting parameter, given by the relaxation time of the dipolar order. The latter, although significant for systems with strong molecular order and immobility, such as lipid bilayers, is expected to be negligible for coagulated milk proteins (Morrison et al., 1995). Hence, these examined models with inclusion of a dipolar reservoir either reduced, or did not improve, the quality of the fit.

Based on the above considerations, we decided to adopt the four-parameter two-pool exchange model, from which the dimensionless composite parameters, *CER* ($R_{ex}M_0^B/R_1^A$) and R_2^A/R_1^A, and the single parameters, T_2^B and R_{ex}, were obtained. The *CER* and R_{ex} are of particular interest for monitoring protein digestion because they describe the ^{1}H protein-water exchange kinetics.

First, the number of measurements at distinct $\omega_1/2\pi$ and Δ values was optimized for obtaining accurate and precise fitting of MT spectra of SM with the two-pool exchange model, yet minimizing the measurement time. We found that reducing the number of saturation pulse powers from seven to three values, namely $\omega_1/2\pi = 1.40$, 0.78 and 0.50 kHz, did not have an effect on the fitting value and error. The optimal values for the saturation pulse power depended on the exchange rate of the sample under study, and for raw SM these values gave the best fit. With 29 offsets, it was possible to include sufficient points in the intermediate offset range while also sampling the two plateaus, which was essential for accurate fitting of the data (Fig. S2 and Table S1).

Next, the MT spectra recorded with the optimized acquisition parameters for raw and heated SM samples at different time points during *in vitro* gastric digestion were fitted with the two-pool exchange model. In general, the fitting successfully described the MT spectra of the digestion samples (Fig. 2 and Fig. S3). However, in a few cases, at $\omega_1/2\pi = 0.5$ kHz and low-frequency offsets, the fitting line deviated from the data. This became more evident for the longer digestion time points, especially from t = 5 min onwards for raw SM. In these cases, a super-Lorentzian line shape provided a better fit than the Gaussian line shape (Fig. S4 and Table S2), but in view of a uniform fitting procedure, we chose to fit all MT spectra with a Gaussian line shape.

Fitting the data with the two-pool exchange model provided plausible values for the model parameters (Fig. 3 and Table S3). The parameters are shown with 95% CIs as derived via bootstrapping. The obtained CIs indicate that all parameters, except R_{ex}, can be obtained with a relative standard error of ≤10%. For R_{ex}, the estimated relative standard error is 10–55%. These errors enable quantitative assessment of the impact of digestion on T_2^B, R_2^A/R_1^A, CER and even R_{ex}. As shown in Fig. 3a, the T_2^B and R_2^A/R_1^A parameter did not notably vary during *in vitro* digestion, but were useful for verifying fitting performance and plausibility of returned values. Since both the T_2^B and R_2^A/R_1^A do not largely vary during *in vitro* digestion, fixing these parameters in the model could be considered for increasing the confidence levels for *CER* and R_{ex}. Indeed, fixing T_2^B and R_2^A/R_1^A to their average value across the digestion duration resulted in a ~2.5 and 4-fold decrease in the error of the *CER* and R_{ex}, respectively. However, a one-way ANOVA revealed that there was still a statistically significant variation over the digestion duration for T_2^B for both raw SM ($F(5,12) = [357.4]$, $P < .001$) and heated SM ($F(5,12) = [59.70]$, $P < .001$).

The same was found for R_2^A/R_1^A for both raw SM ($F(5,12) = [1905]$, $P = <0.001$) and heated SM ($F(5,12) = [2165]$, $P = <0.001$). Therefore, we decided to treat the T_2^B and R_2^A/R_1^A as free parameters in the fitting. The T_2^B remained short, around 14–19 μs, due to the restricted molecular motion of ^{1}H in the coagulum. This is in agreement with the expected short value of T_2^B for semi-solid macromolecules, with 9–20 μs being the range typically reported in the literature, which is too short to be

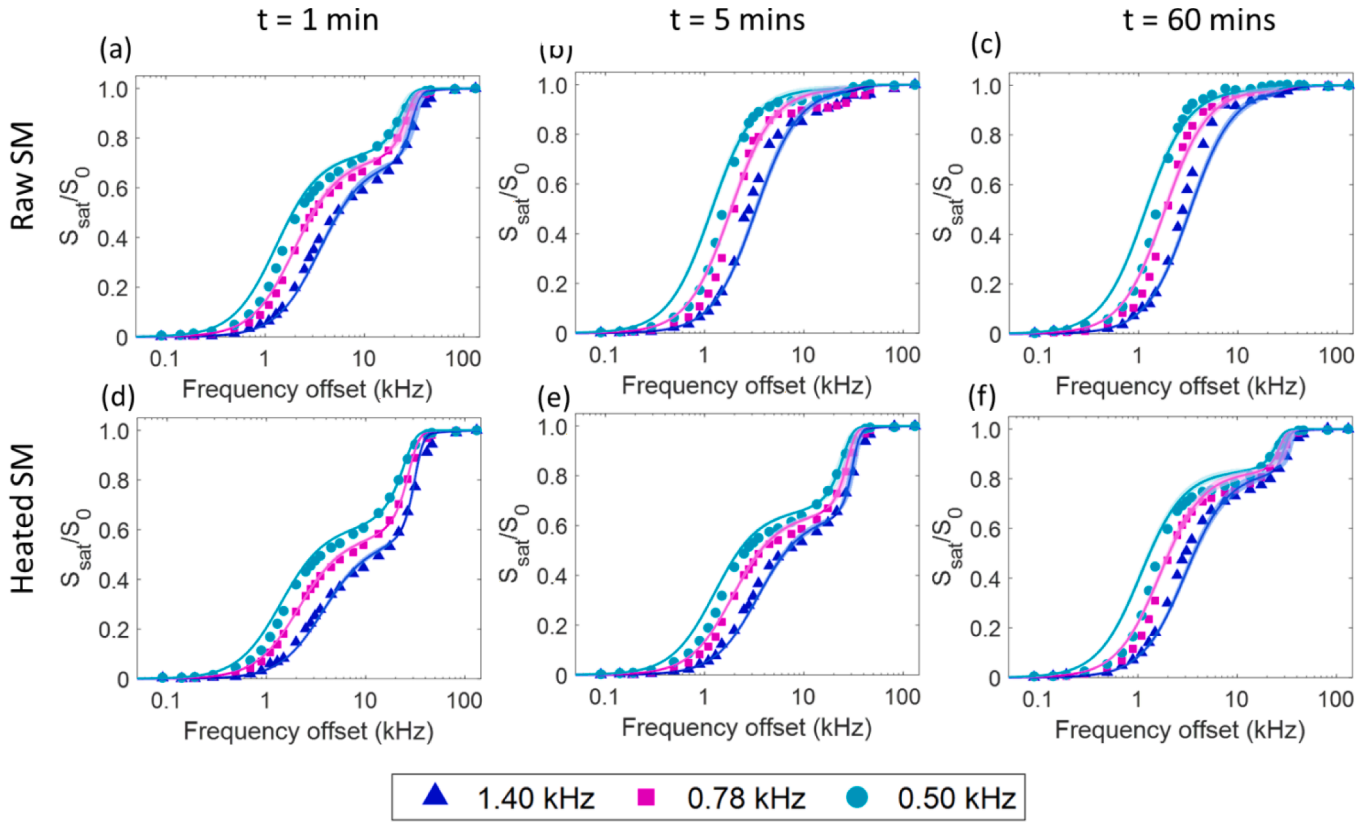

Fig. 2. ^{1}H MT NMR spectra measured with $\omega_1/2\pi = 1.40$, 0.78 or 0.50 kHz for raw skim milk (top panel) or heated skim milk with 90% Whey protein denaturation (bottom panel) digested in the *in vitro* infant gastric digestion model at t = 1 (a and d), t = 5 (b and e) and t = 60 min (c and f). The solid line represents the multiparameter fitting of the two-pool exchange model to the MT data. The thickness of the line represents the 95% confidence intervals that were calculated via bootstrapping (see section 2.6).

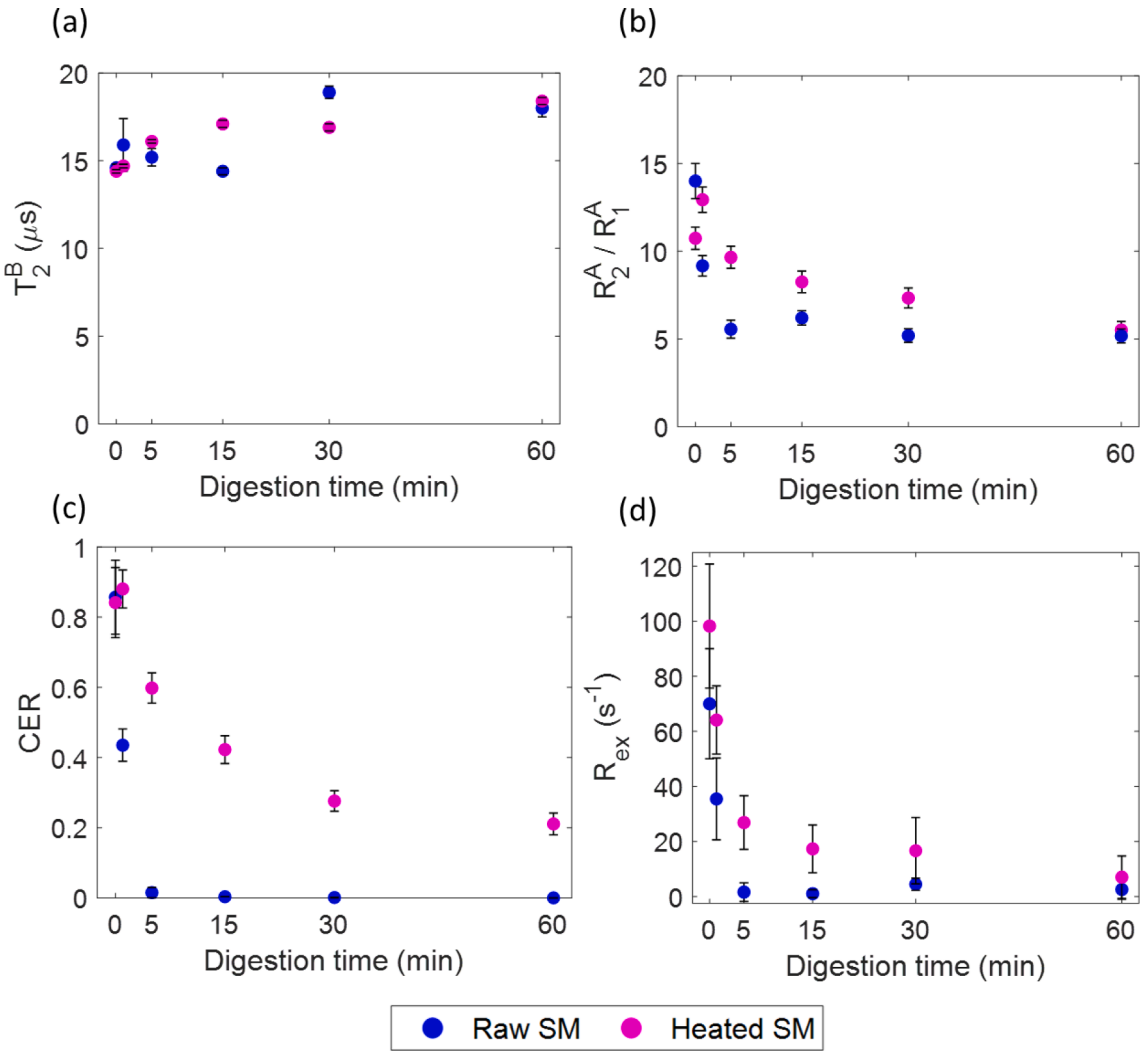

Fig. 3. Evolution of control parameters (a) T_2^B, (b) R_2^A/R_1^A and MT parameters (c) CER and (d) R_{ex} obtained from the multi-parameter fit of the two-pool exchange model to the MT spectra for raw SM and heated SM with 90% WP denaturation during *in vitro* gastric protein digestion. The 95% confidence intervals were calculated via bootstrapping.

measured by conventional NMR (Graham, Stanisz, Kecojevic, Bronskill, & Henkelman, 1999; Jerban et al., 2018). Therefore, the semi-solid protein pool (M_0^B) can only be detected indirectly, by making its signal cross-relax with that of water by, for example, magnetization transfer. The R_2^A/R_1^A ratio is expected to be larger than 1 for water molecules with restricted mobility, which is the case when a large amount of semi-solid protein is present in the sample. For the digestion samples, the R_2^A/R_1^A was between 5 and 13. The mobility of the water molecules is expected to increase during digestion due to a decrease in the amount of coagulum. This explains the decrease observed in the R_2^A/R_1^A from t = 0 to 5 min and t = 0 to 60 min for raw and heated SM, respectively. Both the composite parameter *CER* (Fig. 3c) and the chemical exchange rate R_{ex} (Fig. 3d) increased with the amount of semi-solid proteins present in the sample due to correspondingly more efficient protein-water exchange. The caseins in the coagulum are broken down into insoluble peptides that remain in the coagulum but also soluble peptides that move into the supernatant, thereby leading to a decrease in the *CER* and R_{ex}. While both of these parameters are promising for monitoring protein digestion, the *CER* was determined with a smaller error than R_{ex}. In addition, the *CER* depends not only on the exchange rate but also on the amount of semi-solid protein, which is known to change during protein digestion; furthermore, the *CER* proved comparably more sensitive to heat treatment. Therefore, *CER* will be considered as the most informative MT fitting parameter for studying the breakdown of the protein coagulum.

The *CER* for raw SM largely decreased from t = 0 to 5 min, followed by a plateau towards values close to zero (Fig. 3c). This indicates that most of the breakdown of the casein coagulum occurred within the first 5 min. The *CER* for heated SM increased from t = 0 to t = 1 min followed by a decrease from t = 1 to t = 60 min (Fig. 3c), which is in agreement with the photographs in section 3.1 (Fig. 1b). The *CER* values at all digestion time points were higher for heated SM due to its larger semi-solid protein content compared to raw SM. The observed difference between raw and heated SM in the decrease of *CER* during gastric digestion indicates that heating may cause slower digestion of the protein coagulum. These results show that the *CER* parameter can be used to monitor both *in vitro* gastric digestion and changes in the digestion caused by heating.

3.3. Rapid MT measurements for monitoring digestion

While the *CER* can successfully be used to monitor *in vitro* gastric protein digestion, the experimental conditions required to acquire multiple MT spectra and, thus, estimate *CER*, are not compatible with dynamic studies of *in vivo* protein digestion. This is because the overall measurement time and RF irradiation power respectively exceed the duration of the digestion process itself and the specific absorption rate

(SAR) limitations on clinical MRI scanners. In addition, faster measurements that fit within one breath hold are preferred in order to avoid motion-related artifacts.

Therefore, we explored whether the *CER* could be obtained from a single MT measurement, at a single combination of $\omega_1/2\pi$ and Δ values, if all other parameters in the two-pool exchange model were fixed. The data point at $\omega_1/2\pi = 0.50$ and $\Delta = 7.50$ kHz was chosen because, with this combination, the difference in S_{sat}/S_0 for the different digestion samples was maximized, while the effect of direct saturation of the water signal was minimized. For estimation of the fitting error of *CER*, a Gaussian distribution with 1000 samples of the S_{sat}/S_0 was simulated. The fitting was performed with 1000 repetitions, resulting in 1000 values for the *CER* for each digestion sample from which the 95% CIs were calculated. All other parameters in the model were fixed to their average value across the different digestion time points. The *CER* values obtained from the single-datapoint fit (Fig. 4a) were comparable to the values obtained from the multiparameter fit of 87 data points (Fig. 4b) and, as expected, the fitting error was larger. Overall, the single-datapoint fit of *CER* for both raw (Fig. 4c) and heated (Fig. 4d) SM allows for the assessment of the impact of the digestion time. The larger errors observed for the longer digestion times are in agreement with the results from the multi-parameter global fit (Fig. 2a-c). This approach was based on the assumption that the values of the other model parameters did not significantly affect the outcome of the single-datapoint fit. This was justified because fixing those parameters to other physically realistic values, for example values within the 95% CI obtained from the multiparameter global fitting, did not affect the value of *CER* obtained from the one-datapoint fit. (Fig. S5). This demonstrates that the *CER* can be obtained reliably from a single-shot measurement if all other model parameters are fixed to physically realistic values.

A feasible approach for *in vivo* monitoring of protein digestion is to use the MT ratio (*MTR*), which can simply be calculated as $1 - S_{sat}/S_0$. The *MTR* is semi-quantitative and does not provide information on the chemical exchange kinetics. However, the advantage of using the *MTR* over the *CER* obtained from the one-datapoint fit is that the former does not rely on assumptions nor fitting, and is already an established method for obtaining MT contrast in *in vivo* MRI (Geeraert et al., 2018). The *MTR* and the *CER* both depend on the amount of MT that takes place between the semi-solid protein and the water pool. Therefore, they are expected to follow the same trend during *in vitro* gastric protein digestion. To collect data with optimal MT effect for the digestion samples, the same $\omega_1/2\pi$ and Δ were used as for the single-datapoint fitting approach. The *MTR* for both raw and heated SM decreased with increasing digestion times (Fig. 5a). Higher *MTR* values and a slower variation in the *MTR* were observed for heated SM as compared to raw SM during *in vitro* gastric digestion. These observations are in agreement with the trends observed for the *CER*. However, the variation in the *MTR* for both raw and heated SM was smaller in the first 5 min of *in vitro* gastric digestion, and, in contrast to the *CER* no clear plateau was reached after 5 min for raw SM. Whether *MTR* follows the trend of *CER* depends on the choice of $\omega_1/2\pi$ and Δ. For our selection of these parameters, Pearson correlation coefficient of *MTR* and *CER* showed a significant positive correlation for both raw SM, $r = 0.92$, $n = 5$, $P = 0.001$ and heated SM, $r = 0.95$, $n = 5$, $P = 0.003$. This shows that both parameters follow the same trend and, hence, that the *MTR* can be used as a semi-quantitative alternative for the *CER* to interpret MT contrast in MRI images acquired during gastric protein digestion.

To validate *MTR* as a marker for protein digestion, we benchmarked it against commonly used reference methods, such as the OPA assay, which measures the number of free amino groups, often described as the

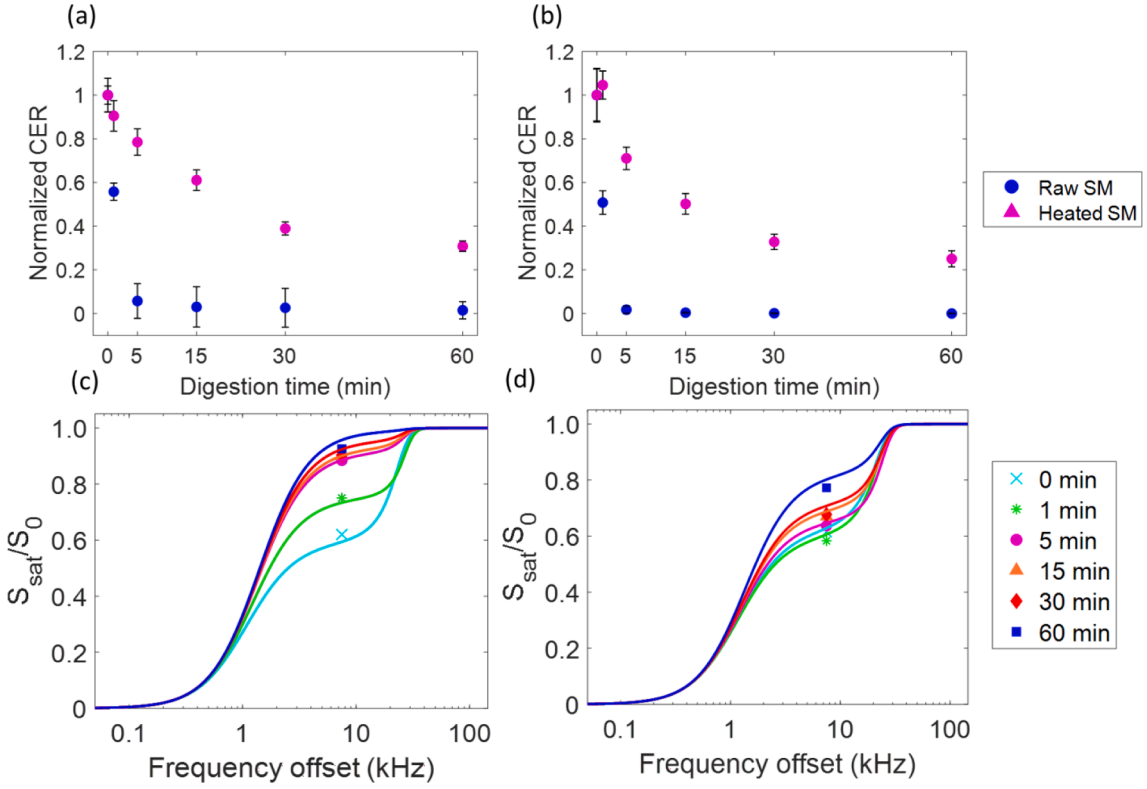

Fig. 4. Evolution of CER during *in vitro* infant gastric digestion obtained from (a) fitting a single-data point at $\omega_1/2\pi = 0.50$ and $\Delta = 7.5$ kHz with the two-pool exchange model in which all parameters except for the CER were fixed to the average value from the multiparameter fit (b) multiparameter global fitting of MT data at $\omega_1/2\pi = 1.40$, 0.78 and 0.50 kHz. Fitting of one datapoint for $\omega_1/2\pi = 0.50$ and $\Delta = 7.5$ kHz for (c) raw and (d) heated SM (90% WP denaturation) at different time points during *in vitro* infant gastric digestion. The CER is normalized to the value at $t = 0$. The error bars in (a) represent the 95% confidence intervals, which were calculated via bootstrapping, in (b) represent the 95% CI interval based on simulating a Gaussian distribution of the single-datapoint with $n = 1000$ and then fitting the simulated datapoints with the two-pool exchange model.

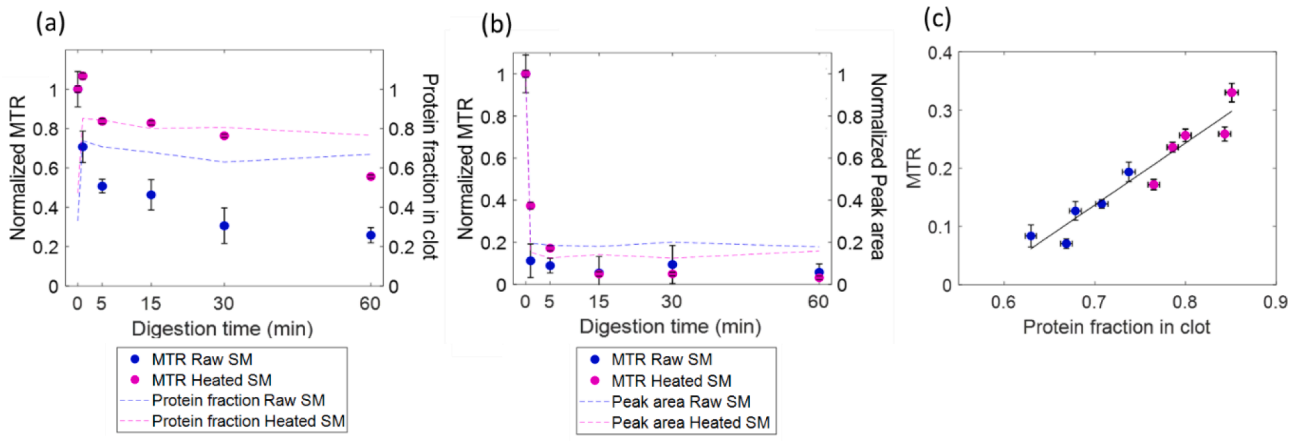

Fig. 5. (a) Evolution of normalized MTR of coagulum and supernatant calculated as $1-S_{sat}/S_0$ for $\omega_1/2\pi = 0.50 \pm 0.05$ kHz and $\Delta = 7.5$ kHz at different time points during *in vitro* infant gastric digestion of raw and heated SM. The protein fraction in the coagulum is plotted in the same figure and was calculated by subtracting the amount of protein in the supernatant determined by DUMAS from the total amount of protein in the sample. (b) normalized MTR of the supernatant and normalized sum of peak areas of caseins determined by RP-HPLC analysis of the supernatant. The MTR and peak areas were normalized to their respective values at t = 0 min. (c) The MTR plotted against the protein fraction in the clot. The Pearson correlation coefficient of the MTR and the protein fraction in the clot for both samples showed a significant positive correlation (r = 0.95, P < .001, n = 10). The first time point, at t = 0 min, has been left out of the correlation analysis.

degree of hydrolysis. This method is mainly applied to study *in vitro* gastric and intestinal digestion in adults (Mulet-Cabero et al., 2019). However, infant gastric digestion is slow due to the low pepsin activity, and the caseins are mainly broken down into relatively large peptides (Ménard et al., 2018). The difference in the number of free amino groups between the intact proteins and large peptides is small and difficult to detect with the OPA assay. In our study, no variation was found in the number of free amino groups during *in vitro* gastric digestion for both raw and heated SM (Fig. S6).

Next, the total protein content and the amount of caseins in the supernatant were determined by DUMAS and RP-HPLC, respectively, generally being used as reference methods. The protein content in the supernatant, as determined by DUMAS, was used to calculate the protein fraction in the coagulum. It should be noted that with DUMAS, as opposed to the Bradford or Bicinchoninic Acid (BCA) assay, the total nitrogen content is measured, which includes also the non-protein nitrogen (NPN) fraction. The NPN in milk mainly consists of urea and makes up only 5% of the total nitrogen. However, because the contribution from the NPN fraction does not vary during protein digestion, DUMAS can be reliably used for protein content analysis of our digestion samples. Furthermore, DUMAS is expected to yield less over-estimation of protein content in milk (Wu, Jackson, Khan, Ahuja, & Pehrsson, 2018) or protein–protein variability (Hayes, 2020) as compared to colorimetric methods. In the results of our DUMAS analysis shown in Fig. 5a, the protein fraction was higher, and the variation during *in vitro* gastric digestion was smaller, for heated SM than for raw SM. The initial protein fraction in the coagulum was smaller than for the subsequent digestion times, because the coagulum at t = 0 min consisted of small flocs that were formed by acid-induced coagulation and the majority of proteins in the sample were at that point still in the supernatant. This was in contrast with the *MTR* and *CER* results, for which the flocs were measured as well and, therefore, contributed to the MT process.

At t = 0 min, the caseins were mainly present as micelles with more exchangeable ^{1}H available than in the casein micelle aggregates that form the coagulum. Therefore, it is expected that the *MTR* and *CER* are highest at t = 0.

The *MTR* results were further benchmarked by comparing the *MTR* of the supernatant (Fig. 5b) with the sum of the peak areas for caseins obtained from RP-HPLC analysis of the supernatant. The *MTR* of the supernatant at t = 1 and 5 min was higher for heated than for raw SM. After 15 min the *MTR* is the same for both raw and heated SM. At t = 1 and 5 min, the supernatant of heated SM contained some coagulated particles, explaining the higher *MTR* measured for those samples. The sum of peak areas of caseins for heated SM were always lower or the same as those for raw SM, indicating that heated SM contained less or the same amount of intact casein in the supernatant as raw SM. A difference was observed between the *MTR* and RP-HPLC analysis for t = 0 and 5 min, which can be explained by the fact that all solid particles had to be removed from the sample for the RP-HPLC analysis, while this was not needed for the *MTR* measurements. As there was nearly no intact casein in the supernatant, RP-HPLC analysis of the supernatant alone is not sufficient to get a complete picture of the digestion.

Overall, the MT results are in agreement with the reference methods and a positive significant correlation was found between the *MTR* and protein fraction in the clot (r = 0.95, *P* < 001, n = 10; Fig. 5c). It should be noted that an additional advantage of the MT-NMR methods is that the *MTR* is more sensitive to gastric protein digestion compared to protein content measurements. The decrease in the *MTR* between t = 1 min and 60 min is 60% and 45% for raw and heated SM, respectively, while the corresponding decrease in the protein content is 10% for both milk samples.

The MT results are further supported by previous observations (Sánchez-Rivera, Ménard, Recio, & Dupont, 2015) of a difference in casein digestion kinetics between raw and heated SM. Sánchez-Rivera and co-workers found a decrease in caseins after 4 min of digestion of 80% and 8%, respectively for raw and heated SM. This is comparable with the *MTR* and *CER* results in our study. The decrease in the *MTR* was 50% and 10%, and the decrease in the *CER* was 90% and 20% for raw and heated SM, respectively. Heating can cause the caseins and denatured whey protein to aggregate together, thereby leading to slower pepsin penetration of the coagulum, which may explain the slower gastric digestion of the protein coagulum in heated SM.

In this work, we focused solely on gastric digestion because it is the first step in the digestion process, and it is well known to be affected by heat treatment. Protein digestion continues in the intestines, where the solubilized proteins and relatively large peptides, produced during gastric digestion, are further hydrolyzed into small peptides and amino acids that can be absorbed.

Gastric digestion may have an influence on intestinal digestion, and thereby on subsequent absorption of small peptides and amino acids (Mulet-Cabero, Mackie, Brodkorb, & Wilde, 2020). In future works, it would be interesting to link the effect of processing on gastric digestion to the absorption of peptides and amino acids.

Our results show that ^{1}H MT NMR can be used to monitor *in vitro*

protein digestion and that the *MTR* is a promising marker for monitoring *in vivo* gastric protein digestion in humans. The current duration of the *MTR* measurements is 2.6 min, but this could be further reduced by reducing the saturation pulse length and the number of scans, to make the measurement fit within one breath hold. The next step will be to assess the capability of MT to monitor protein digestion under conditions more similar to *in vivo* digestion, *e.g.* by using a dynamic *in vitro* digestion model.

4. Conclusions

^{1}H MT NMR was successfully applied, and benchmarked against reference methods, to non-invasively study *in vitro* gastric protein digestion of raw and heated SM. The MT spectra are sensitive to changes in the ^{1}H protein-water exchange kinetics, which occurred during protein digestion. The quantitative composite parameter, *CER*, can be determined as a function of digestion time with a relative standard error of $\leq$10%, both by MT spectra and single-point MT measurements. The decrease in the *CER* is in line with the literature and reference data of *in vitro* gastric digestion of SM. Therefore, the *CER* is a suitable parameter for monitoring *in vitro* gastric protein digestion. For a more rapid MT measurement that does not require data fitting, the semi-quantitative *MTR* can be used, which is more feasible for *in vivo* studies on clinical MRI systems. Heating of SM results in a slower decrease of the *CER* and *MTR* with digestion, indicating a difference in protein coagulum digestion kinetics between heated and raw SM. Therefore, MT could also be applied to study the effect of processing on protein digestion. Our results pave the way for future *in vivo* quantification of protein digestion by means of MT-MRI.

CRediT authorship contribution statement

Morwarid Mayar: Conceptualization, Investigation, Methodology, Validation, Writing – original draft. **Julie L. Miltenburg:** Investigation, Validation. **Kasper Hettinga:** Funding acquisition, Writing – review & editing. **Paul A.M. Smeets:** Conceptualization, Writing – review & editing. **John P.M. van Duynhoven:** Conceptualization, Writing – review & editing. **Camilla Terenzi:** Conceptualization, Methodology, Writing – review & editing.

Declaration of Competing Interest

The authors declare the following financial interests/personal relationships which may be considered as potential competing interests: John van Duynhoven reports financial support was provided by Unilever Food Innovation Centre. Morwarid Mayar reports financial support was provided by TKI agri&food. Julie Miltenburg reports financial support was provided by TKI agri&food. John van Duynhoven reports a relationship with Unilever Food Innovation Centre that includes: employment.

Acknowledgements

Gert-Jan Goudappel is gratefully acknowledged for providing the MT-NMR pulse sequence and for his help with setting up the measurements. We thank Dirk Wevers for his contribution to optimizing the MT acquisition parameters. Ewoud van Velzen is gratefully acknowledged for his expert advice on modelling and bootstrapping. Camilla Terenzi acknowledges funding from the 4TU Precision Medicine program supported by High Tech for a Sustainable Future, a framework commisioned by the four Universities of Technology of the Netherlands. We also acknowledge the support of NWO for the MAGNEFY centre, which is part of the uNMR-NL national facility.

Source of funding

This research is part of a public-private partnership project that is financially supported by the Dutch Ministry of Economic Affairs; TKI-AF grant no. AF-18012 (Digestion & immunogenicity of proteins in infant nutrition).

Appendix A. Supplementary data

Supplementary data to this article can be found online at https://doi.org/10.1016/j.foodchem.2022.132545.

References

Bordoni, A., Picone, G., Babini, E., Vignali, M., Danesi, F., Valli, V., … Capozzi, F. (2011). NMR comparison of in vitro digestion of Parmigiano Reggiano cheese aged 15 and 30 months. *Magnetic Resonance in Chemistry, 49*, 61–70. https://doi.org/10.1002/mrc.2847

Bornhorst, G. M., & Paul Singh, R. (2014). Gastric digestion in vivo and in vitro: How the structural aspects of food influence the digestion process. *Annual Review of Food Science and Technology, 5*(1), 111–132. https://doi.org/10.1146/annurev-food-030713-092346

Brodkorb, A., Egger, L., Alminger, M., Alvito, P., Assunção, R., Ballance, S., … Recio, I. (2019). INFOGEST static in vitro simulation of gastrointestinal food digestion. *Nature Protocols, 14*(4), 991–1014. https://doi.org/10.1038/s41596-018-0119-1

Ceckler, T., Maneval, J., & Melkowits, B. (2001). Modeling magnetization transfer using a three-pool model and physically meaningful constraints on the fitting parameters. *Journal of Magnetic Resonance, 151*(1), 9–27. https://doi.org/10.1006/jmre.2001.2326

Chinachoti, P., Vittadini, E., Chatakanonda, P., & Vodovotz, Y. (2008). Characterization of molecular mobility in carbohydrate food systems by NMR. In G. A. Webb (Ed.), *Modern magnetic resonance* (pp. 1703–1712). Dordrecht: Springer. https://doi.org/10.1007/1-4020-3910-7_191.

de Vries, R., van Knegsel, A., Johansson, M., Lindmark-Månsson, H., van Hooijdonk, T., Holtenius, K., & Hettinga, K. (2015). Effect of shortening or omitting the dry period of Holstein-Friesian cows on casein composition of milk. *Journal of Dairy Science, 98*(12), 8678–8687. https://doi.org/10.3168/jds.2015-9544

De Zwart, I. M., & De Roos, A. (2010). MRI for the evaluation of gastric physiology. *European Radiology, 20*(11), 2609–2616. https://doi.org/10.1007/s00330-010-1850-3

Deng, R., Janssen, A. E. M., Vergeldt, F. J., Van As, H., de Graaf, C., Mars, M., & Smeets, P. A. M. (2020). Exploring in vitro gastric digestion of whey protein by time-domain nuclear magnetic resonance and magnetic resonance imaging. *Food Hydrocolloids, 99*(2019), 105348–105358. https://doi.org/10.1016/j.foodhyd.2019.105348

Dupont, D., Alric, M., Blanquet-Diot, S., Bornhorst, G., Cueva, C., Deglaire, A., … Van den Abbeele, P. (2019). Can dynamic in vitro digestion systems mimic the physiological reality? *Critical Reviews in Food Science and Nutrition, 59*(10), 1546–1562. https://doi.org/10.1080/10408398.2017.1421900

Dupont, D., & Tomé, D. (2014). Milk proteins: Digestion and absorption in the gastrointestinal tract. In M. Boland, & H. Singh (Eds.), *Milk proteins from expression to food* (3rd ed., pp. 701–714). Cambridge Massachusetts: Academic Press. https://doi.org/10.1016/B978-0-12-405171-3.00020-9.

Efron, B., & Tibshirani, R. J. (Eds.). (1993). *An introduction to the bootstrap*. Boston, MA: Springer US.

Egger, L., Ménard, O., Baumann, C., Duerr, D., Schlegel, P., Stoll, P., … Portmann, R. (2019). Digestion of milk proteins: Comparing static and dynamic in vitro digestion systems with in vivo data. *Food Research International, 118*(December 2017), 32–39. 10.1016/j.foodres.2017.12.049.

Geeraert, B. L., Lebel, R. M., Mah, A. C., Deoni, S. C., Alsop, D. C., Varma, G., & Lebel, C. (2018). A comparison of inhomogeneous magnetization transfer, myelin volume fraction, and diffusion tensor imaging measures in healthy children. *NeuroImage, 182*(2017), 343–350. https://doi.org/10.1016/j.neuroimage.2017.09.019

Graham, S. J., Stanisz, G. J., Kecojevic, A., Bronskill, M. J., & Henkelman, R. M. (1999). Analysis of changes in MR properties of tissues after heat treatment. *Magnetic Resonance in Me, 42*(6), 1061–1071. https://doi.org/10.1002/(SICI)1522-2594(199912)42:6<1061::AID-MRM10>3.0.CO;2-T

Guo, J., Erickson, R., Trouard, T., Galons, J.-P., & Gillies, R. (2003). Magnetization transfer contrast imaging in Niemann pick type C mouse liver. *Journal of Magnetic Resonance Imaging, 18*(3), 321–327. https://doi.org/10.1002/jmri.10404

Hayes, M. (2020). Measuring protein content in food: An overview of methods. *Foods, 9*(10), 1340. https://doi.org/10.3390/foods9101340

Henkelman, R. M., Huang, X., Xiang, Q.-S., Stanisz, G. J., Swanson, S. D., & Bronskill, M. J. (1993). Quantitative interpretation of magnetization transfer. *Magnetic Resonance in Medicine, 29*(6), 759–766. https://doi.org/10.1002/mrm.1910290607

Henkelman, R. M., Stanisz, G. J., & Graham, S. J. (2001). Magnetization transfer in MRI: A review. *NMR in Biomedicine, 14*(2), 57–64. https://doi.org/10.1002/nbm.683

Jerban, S., Ma, Y., Nazaran, A., Dorthe, E. W., Cory, E., Carl, M., … Du, J. (2018). Detecting stress injury (fatigue fracture) in fibular cortical bone using quantitative ultrashort echo time-magnetization transfer (UTE-MT): An ex vivo study. *NMR in Biomedicine, 31*(11), e3994. https://doi.org/10.1002/nbm.3994

Le Dean, A., Mariette, F., & Marin, M. (2004). 1H nuclear magnetic resonance relaxometry study of water state in milk protein mixtures. *Journal of Agricultural and Food Chemistry, 52*(17), 5449–5455. https://doi.org/10.1021/jf030777m

Macierzanka, A., Böttger, F., Lansonneur, L., Groizard, R., Jean, A.-S., Rigby, N. M., … Mackie, A. R. (2012). The effect of gel structure on the kinetics of simulated gastrointestinal digestion of bovine β-lactoglobulin. *Food Chemistry, 134*(4), 2156–2163. https://doi.org/10.1016/j.foodchem.2012.04.018

Ménard, O., Bourlieu, C., De Oliveira, S. C., Dellarosa, N., Laghi, L., Carrière, F., … Deglaire, A. (2018). A first step towards a consensus static in vitro model for simulating full-term infant digestion. *Food Chemistry, 240*(2017), 338–345. https://doi.org/10.1016/j.foodchem.2017.07.145

Morrison, C., Stanisz, G., & Henkelman, R. M. (1995). Modeling magnetization transfer for biological-like systems using a semi-solid pool with a super-Lorentzian lineshape and dipolar reservoir. *Journal of Magnetic Resonance, 108*(2), 103–113. https://doi.org/10.1006/jmrb.1995.1111

Mulet-Cabero, A. I., Mackie, A. R., Brodkorb, A., & Wilde, P. J. (2020). Dairy structures and physiological responses: A matter of gastric digestion. *Critical Reviews in Food Science and Nutrition, 60*(22), 3737–3752. https://doi.org/10.1080/10408398.2019.1707159

Mulet-Cabero, A. I., Mackie, A. R., Wilde, P. J., Fenelon, M. A., & Brodkorb, A. (2019). Structural mechanism and kinetics of in vitro gastric digestion are affected by process-induced changes in bovine milk. *Food Hydrocolloids, 86*, 172–183. https://doi.org/10.1016/j.foodhyd.2018.03.035

Nakai, S., & Li-Chan, E. (1987). Effect of clotting in stomachs of infants on protein digestibility of milk. *Food Structure, 6*(2), 161–170.

Sánchez-Rivera, L., Ménard, O., Recio, I., & Dupont, D. (2015). Peptide mapping during dynamic gastric digestion of heated and unheated skimmed milk powder. *Food Research International, 77*, 132–139. https://doi.org/10.1016/j.foodres.2015.08.001

Sinclair, C. D. J., Samson, R. S., Thomas, D. L., Weiskopf, N., Lutti, A., Thornton, J. S., & Golay, X. (2010). Quantitative magnetization transfer in in vivo healthy human skeletal muscle at 3 T. *Magnetic Resonance in Medicine, 64*(6), 1739–1748. https://doi.org/10.1002/mrm.22562

Sled, J. G. (2018). Modelling and interpretation of magnetization transfer imaging in the brain. *NeuroImage, 182*(2017), 128–135. https://doi.org/10.1016/j.neuroimage.2017.11.065

Smeets, P. A. M., Deng, R., Van Eijnatten, E. J. M., & Mayar, M. (2020). Monitoring food digestion with magnetic resonance techniques. *Proceedings of the Nutrition Society, 3*, 1–11. https://doi.org/10.1017/S0029665120007867

Spiller, R., & Marciani, L. (2019). Intraluminal impact of food: New insights from MRI. *Nutrients, 11*(5), 1147–1161. https://doi.org/10.3390/nu11051147

van Duynhoven, J. P. M., Kulik, A. S., Jonker, H. R. A., & Haverkamp, J. (1999). Solid-like components in carbohydrate gels probed by NMR spectroscopy. *Carbohydrate Polymers, 40*(3), 211–219. https://doi.org/10.1016/S0144-8617(99)00056-9

Duynhoven, J. van, Voda, A., Witek, M., & Van As, H. B. T. (2010). Chapter 3 - Time-domain NMR applied to food products (Vol. 69, pp. 145–197). Academic Press. 10.1016/S0066-4103(10)69003-5.

van Lieshout, G. A. A., Lambers, T. T., Bragt, M. C. E., & Hettinga, K. A. (2020). How processing may affect milk protein digestion and overall physiological outcomes: A systematic review. *Critical Reviews in Food Science and Nutrition, 60*(14), 2422–2445. https://doi.org/10.1080/10408398.2019.1646703

Van Zijl, P. C. M., Zhou, J., Mori, N., Payen, J. F., Wilson, D., & Mori, S. (2003). Mechanism of magnetization transfer during on-resonance water saturation. A new approach to detect mobile proteins, peptides, and lipids. *Magnetic Resonance in Medicine, 49*(3), 440–449. https://doi.org/10.1002/mrm.10398

Vlaardingerbroek, M. T., & den Boer, J. A. (2003). *Magnetic resonance imaging: Theory and practice* (3rd ed.). Berlin Heidelberg: Springer-Verlag, Berlin Heidelberg.

Walstra, P., Wouters, J. T. M., & Geurts, T. J. (2006). *Dairy science and technology* (2nd ed.). Boca Raton, FL: CRC Press.

Wu, X., Jackson, R. T., Khan, S. A., Ahuja, J., & Pehrsson, P. R. (2018). Human milk nutrient composition in the United States: Current knowledge, challenges, and research needs. *Current Developments in Nutrition, 2*(7), 1–18. https://doi.org/10.1093/cdn/nzy025